Angewandte
International Edition Chemie

Catalytic Oxidation

DOI: 10.1002/anie.201205018

Water Oxidation by Single-Site Ruthenium Complexes: Using Ligands as Redox and Proton Transfer Mediators**

*Markus D. Kärkäs, Torbjörn Åkermark, Eric V. Johnston, Shams R. Karim, Tanja M. Laine, Bao-Lin Lee, Tobias Åkermark, Timofei Privalov, and Björn Åkermark**

The splitting of water into molecular oxygen and hydrogen gas is an attractive option for the production of sustainable energy. The process of oxidizing water is the key step for realizing this goal. The possibilities are enormous, as the hydrogen can be used as a fuel, stored for future demands, or even used for the production of more complex fuels and chemicals.[1] The challenge is that the splitting of water requires both a relatively large input of energy, $E° = 1.23$ V versus normal hydrogen electrode (NHE; at pH 0), and a catalyst that allows the reaction to proceed at a reasonable rate. In Nature, light-driven water oxidation is carried out by a tetranuclear manganese cluster,[2] located in the oxygen evolving complex (OEC), at a rate which we are only now starting to approach with synthetic mimics. To facilitate mechanistic studies, these mimics generally consist of well-defined molecular water oxidation catalysts (WOCs) containing one or several high-valent redox-active metals in the center. Intensive efforts during recent years have resulted in the development of a number of mono- and dinuclear Ru-,[3] Ir-,[4] Mn-,[5] Co-[6] and Fe-based[7] complexes.

A major drawback is that most of the catalysts developed thus far require a powerful sacrificial oxidant (Ce^{IV}), to oxidize water. However, for the development of a sustainable water splitting system, the oxidant needs to be a light-absorbing component (a photosensitizer), which can be regenerated. A major obstacle frequently encountered in light-driven water oxidation is the mismatch between the relatively high redox potential at which a catalyst assumes its active state and the lower potential attainable with a photosensitizer. One way to decrease the redox potential is to involve proton-coupled electron transfer (PCET), which is a fundamental process in Nature.[8] It involves simultaneous transfer of an electron and a proton and has a profound influence on mechanisms and energetics of chemical reactions. Therefore, PCET can allow for the accumulation of multiple redox equivalents, a prerequisite for carrying out multi-electron reactions. Another way to affect the redox potential of the system is to attach electron-donating and redox-active ligands to the metal centers. This would also influence the balance between efficiency and stability of the WOCs.

It seemed plausible that the introduction of imidazole and phenol motifs, in combination with carboxylate groups, could facilitate proton coupled reactions and result in WOCs with the ability to form high-valent metal–oxo species at low potentials. Therefore, the meridionally coordinating benzimidazole based ligands **1** and **2**, and the related single-site ruthenium complexes **3** and **4** were synthesized (Scheme 1; see the Supporting Information for further details). Ligands **1** and **2** both contain imidazole and phenol motifs, which are important components in the natural system. In fact, by using the imidazole motif, it was possible to introduce a combined redox and proton transfer mediator, a highly active and essential element, into these single-site ruthenium WOCs. With complex **3** in particular, we were able to reliably reach turnover numbers (TONs) and initial turnover frequencies (TOFs), of up to 4000 and $>7\,s^{-1}$, respectively, with $[Ru(bpy)_3]^{3+}$ as the oxidant; to the best of our knowledge, these are the highest values reported for any metal-based water oxidation catalyst. Also, $[Ru^{V}{=}O]^{n+}$, the postulated active key intermediate in water oxidation was successfully characterized by high-resolution mass spectrometry (HRMS).

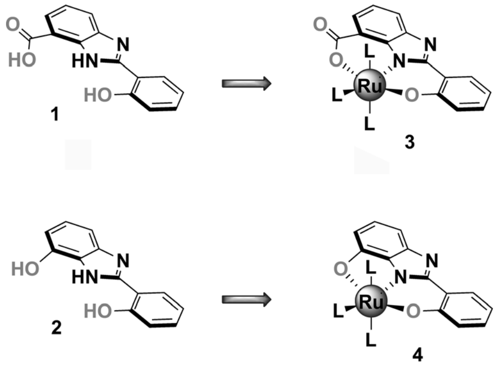

Scheme 1. Molecular structures of ligands **1** and **2** and the single-site ruthenium complexes **3** and **4**. L = 4-picoline.

The single-site ruthenium complexes **3** and **4** were synthesized according to Figure S1 (see the Supporting Information). To study the oxidation of water with a chemical oxidant, water oxidation catalyzed by complexes **3** and **4** was

---

[*] M. D. Kärkäs, T. Åkermark, Dr. E. V. Johnston, S. R. Karim, T. M. Laine, B.-L. Lee, Prof. T. Privalov, Prof. B. Åkermark
Department of Organic Chemistry, Arrhenius Laboratory
Stockholm University, 10691 Stockholm (Sweden)
E-mail: bjorn.akermark@organ.su.se
Dr. T. Åkermark
Department of Materials and Environmental Chemistry
Arrhenius Laboratory, Stockholm University
10691 Stockholm (Sweden)

[**] Financial support from the Swedish Energy Agency and the Knut and Alice Wallenberg Foundation is gratefully acknowledged.

Supporting information for this article, including detailed synthetic methods and procedures, characterization, and quantum chemical calculations, is available on the WWW under http://dx.doi.org/10.1002/anie.201205018.

first evaluated with $[Ru(bpy)_3]^{3+}$. Upon addition of an aqueous phosphate buffer solution of catalyst **3** or **4** to $[Ru(bpy)_3]^{3+}$, immediate O_2 evolution was observed (Figure 1 a,b, respectively). In the absence of catalyst **3** or **4** only negligible amounts of O_2 were detected, if any. A series of experiments were conducted and it was revealed that catalyst **3** was a highly efficient catalyst for water oxidation. With a concentration of 33 nM of catalyst **3** and 10 mM $[Ru(bpy)_3]^{3+}$, a turnover number (TON, $n_{O_2}/n_{catalyst}$) of 4000 was obtained within 15 min. The initial turnover frequency was calculated to be $>7\,s^{-1}$ (Supporting Information, Table S1), which is among the highest reported for any catalytic system employing a chemical oxidant (regardless of whether Ce^{IV} or $[Ru(bpy)_3]^{3+}$ was employed as the oxidant). Experiments conducted with catalyst **4** resulted in a considerably lower TON, perhaps because of the fact that it is more sensitive to oxidation. The final yields of evolved O_2 based upon $[Ru(bpy)_3]^{3+}$ $(4n_{O_2}/n_{[Ru(bpy)_3]^{3+}})$ were calculated to be 53, 27, 14, and 5.2% for catalyst **3**, at 33, 3.3, 0.33, and 0.033 µM, respectively. For catalyst **4**, the yields were determined to be 52, 6.5, and 2.2% at 33, 3.3, and 0.33 µM, respectively. However, at lower pH, the use of $[Ru(bpy)_3]^{3+}$ as an oxidant results in inefficient catalytic H_2O oxidation.

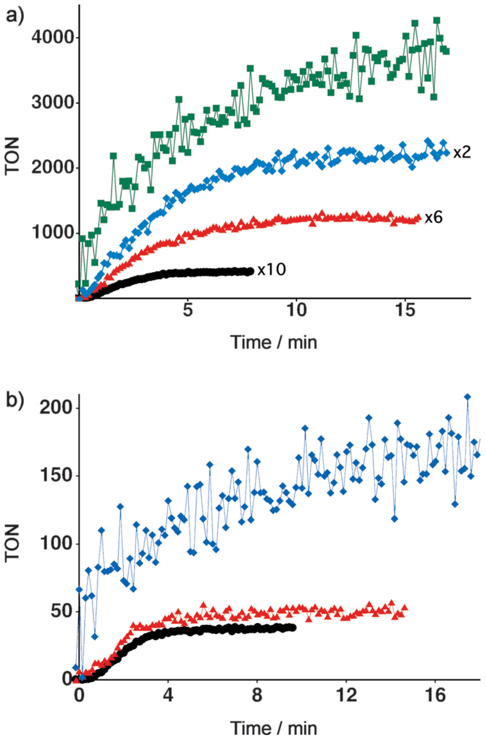

Figure 1. Chemical water oxidation catalyzed by a) complex **3** and b) complex **4** using $[Ru(bpy)_3]^{3+}$ as an oxidant. Conditions: A deoxygenated aqueous phosphate buffer solution (0.1 M, pH 7.2, 0.5 mL) of catalyst **3** or **4** was added to $[Ru(bpy)_3](PF_6)_3$ (5.1 mg, 5.1 µmol). 33 µM (●), 3.3 µM (▲), 0.33 µM (◆), 0.033 µM (■).

If photochemically generated $[Ru(bpy)_3]^{3+}$ is to replace Ce^{IV}, the redox potentials of the catalysts have to be decreased from ca. 1.6–1.7 V to < 1.4 V vs. NHE. At present, only a few reported complexes have been reported which catalyze water oxidation at the potential generated by $[Ru(bpy)_3]^{2+}$, 1.26 V vs. NHE (see Table 1). This table clearly demonstrates that complex **3** stands out from the rest.

Table 1: Comparison of TONs for different WOCs utilizing $[Ru(bpy)_3]^{3+}$ as an oxidant.

Complex	TON[a]	Reference
3	4000 (4000)	this work
4	180 (180)	this work
$[\{Ru_4O_4(OH)_2(H_2O)_4\}(\gamma\text{-}SiW_{10}O_{36})_2]^{10-}$	18 (4.5)	Ref. [9]
$[Ru(bda)(pic)_2]$	30 (30)	Ref. [10]
$[Co_4(H_2O)_2(PW_9O_{34})_2]^{10-}$	1000 (250)	Ref. [6b]

[a] TON = n_{O_2}/n_{cat}; numbers in parentheses are [TON/unit metal]. bda = 2,2′-bipyridine-6,6′-dicarboxylate, pic = 4-picoline.

To evaluate the possibility of carrying out light-driven water oxidation under homogeneous, neutral conditions (pH 7.2), a system consisting of catalyst **3** or **4**, a photosensitizer ($[Ru(bpy)_3]^{2+}$ or $[Ru(bpy)_2(deeb)]^{2+}$; deeb = 4,4′-di(ethoxycarbonyl)-2,2′-bipyridine) and a sacrificial electron acceptor ($Na_2S_2O_8$) was employed. This is a well-studied reaction, which proceeds by quenching of the Ru^{II} sensitizer to give the Ru^{III} oxidant and a SO_4^{-} radical, which generates a second molecule of Ru^{III}. The Ru^{III} complexes then oxidize the WOC, which in turn oxidizes water to oxygen.[11] A curious fact is that although the SO_4^{-} radical has a very high oxidation potential ($E° = 2.4$ V vs. NHE), there is at least another clear example showing that negligible amounts of oxygen are formed by direct oxidation of the WOC by the sulfate radical in the presence of an excess of sensitizer (see the Supporting Information).[3j] Evolution of molecular oxygen was detected upon illumination of this three component system. Figure S4 displays the kinetics of oxygen evolution measured by mass spectrometry (MS) of a phosphate buffer solution (0.1 M, pH 7.2) containing catalyst **3** or **4**, a photosensitizer, and the acceptor. In the presence of the $[Ru(bpy)_3]^{2+}$ photosensitizer low TONs of ca. 20 were obtained for catalysts **3** and **4**. The photocatalytic system was therefore evaluated with $[Ru(bpy)_2(deeb)]^{2+}$ as the photosensitizer. Replacing $[Ru(bpy)_3]^{2+}$ (E $[Ru^{III}/Ru^{II}] = 1.26$ V vs. NHE) by the more strongly oxidizing photosensitizer $[Ru(bpy)_2(deeb)]^{2+}$ (E $[Ru^{III}/Ru^{II}] = 1.4$ V vs. NHE) a significantly higher TON of close to 200 could be reached for complexes **3** and **4** (Figure S4). When diluting the concentration to 1 µM for complex **3**, a TON of 300 was obtained under otherwise unchanged conditions (not shown). A series of control experiments confirmed that catalyst, photosensitizer, persulfate, and photons are all necessary to achieve O_2 evolution. These findings confirm that catalyst **3** or **4** is required to achieve visible-light-induced water oxidation.

The origin of the O atoms in the evolved O_2 was investigated by employing isotopically labeled water ($H_2{}^{18}O$) and then measuring the enriched O_2 by MS (Figures S5 and S6). Using a relative concentration of ^{18}O of 7%, the relative abundance of the different oxygen isotopes $^{18,18}O_2$, $^{16,18}O_2$, and $^{16,16}O_2$ ($m/z = 6$, 34 and 32) were recorded and analyzed. The theoretical values, assuming that both oxygen atoms are derived from H_2O, were calculated for the different isotopes. The relative abundance of the different oxygen isotopes is in agreement with the calculated values for both complexes. These results clearly demonstrate that H_2O is the source of oxygen in the evolved O_2, a question which has been of major concern with previously reported water oxidation catalysts.[12]

The ^{1}H NMR spectra in [D$_4$]MeOH of complexes **3** and **4** showed the characteristics of paramagnetic compounds and displayed broad signals. Upon the addition of ascorbic acid, which reduces the ruthenium(III) complexes to ruthenium(II), the complexes could be characterized by ^{1}H NMR, thus confirming the structures of complexes **3** and **4** (Figures S2 and S3, respectively). Analysis of the ruthenium(III) complex **3** by HRMS, in positive mode, displayed three signals at $m/z = 633.1320$, 540.0727, and 447.0160, which correspond to the monocationic species $[\mathbf{3}+H^+]^+$, $[\mathbf{3}-L+H^+]^+$, and $[\mathbf{3}-2L+H^+]^+$ (L = 4-picoline; Figure S7a–c), respectively. For complex **4**, three signals were similarly observed at $m/z =$ 605.1372, 512.0781, and 419.0210, which were assigned to $[\mathbf{4}+H^+]^+$, $[\mathbf{4}-L+H^+]^+$ and $[\mathbf{4}-2L+H^+]^+$, respectively (Figure S7d–f).

The calculated structures of the mononuclear ruthenium complexes **3** and **4** with either the 4-picoline or water coordinated at the equatorial position are shown in Figure 2 and in Figure S21, respectively.[13] Since ligands **1** and **2** both have a charge of −3, the Ru^{III} complexes are neutral overall. If reduced to the Ru^{II} state, complexes with a protonated imidazole fragment are neutral overall (shown in Figure S18). It has been emphasized in the literature that ease of access of a water molecule to the ruthenium center is a prerequisite for an efficient WOC. In the aqueous media described within the self-consistent solvent model, complexes **3** and **4** with a coordinating picoline were calculated to be more stable than the water-coordinating analogues. According to our calculations, the equatorial picoline-water ligand exchange was calculated to be endothermic by about 5 kcal mol^{-1} in the ruthenium(III) state. To verify this, spectrophotometric titration of the two ruthenium(III) complexes was conducted. The spectral changes upon the gradual addition of water to a solution of complex **3** or **4** were monitored by UV/Vis spectroscopy (at $\lambda = 400$ nm; Figures S9–S12). The solvolysis equilibrium constants were calculated to be 0.29 and 0.43 for **3** and **4**, respectively, which indicate that the picoline–water exchange should be facile.

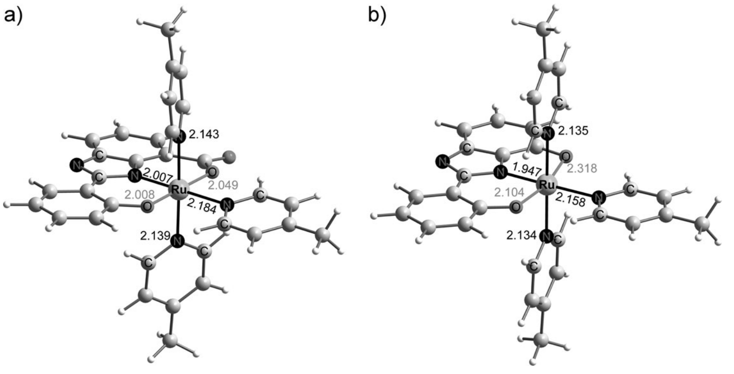

Figure 2. DFT-calculated structures of the mononuclear ruthenium complexes a) **3** and b) **4** with 4-picoline ligands. Distances shown are in Å.

Solid samples of complexes **3** and **4** were analyzed by electron paramagnetic resonance (EPR) at 298 K (Figure S27 a,b). Both are ruthenium(III) complexes with low-spin d^5, $S = ^1/_2$, and have g values of 2.18 and 2.14, for complexes **3** and **4**, respectively. These values are relatively low for ruthenium(III) complexes and suggest that the electron in the singly occupied molecular orbital (SOMO) of the complexes is partly ligand centered and there is a considerable ligand spin delocalization existing in both complexes, which is further supported by DFT calculations (Figure S27c,d). In the complexes ruthenium has a d^5 configuration, although the Mulliken spin population of the ruthenium is about 0.7, not exactly 1, because of delocalization of the SOMO to the ligand. The spin density distribution, shown in Figure S27 c,d, is thus metal-centered, with strong contributions from the ligand (see also, Figures S20 and S21).[14]

The electronic absorption spectra of the two mononuclear ruthenium(III) complexes in an aqueous solution display intense absorption bands in the near-UV region of 300–400 nm (Figure S8), which are assigned to π–π* transitions in the ligands. Indeed, the π system appears to be involved in the HOMOs and LUMOs, as well as the total spin densities (Figures S18, S20, and S21). The absorption at about 390 nm and 370 nm corresponds to electronic transitions with energies close to the HOMO–LUMO gap.

The electrochemistry of complexes **3** and **4** was studied by cyclic voltammetry (CV) and differential pulse voltammetry (DPV) in an aqueous solution of phosphoric acid at pH 1.0 (Figures S13 and S14) and in an aqueous phosphate buffer (0.1 M, pH 7) solution (Figure S15). Both complexes exhibited an electrocatalytic wave for water oxidation with an onset potential of ca. 1.4 V vs. NHE. At pH 7 the onset potential was significantly decreased to ca. 1.24 V vs. NHE for the two complexes. By introducing the negatively charged ligands **1** and **2**, the redox potentials for complexes **3** and **4** were dramatically decreased compared to complexes containing neutral ligands.[3b] The electrochemical data for the two ruthenium complexes in aqueous media is summarized in Table S4 and the calculated structures of plausible complexes are shown in Figures S19, S21s, and S23–S25. To obtain further insight into the electrochemical pH dependence of complex **3**, a Pourbaix diagram was constructed. All three oxidation steps, from ruthenium(II) to ruthenium(V) displayed a pH dependence with a slope of 59 mV/pH, indicating a dependence on the removal of a proton in the one-electron redox processes (Figure S16 and Scheme 2).

The observation and characterization of active intermediates during water oxidation catalysis is of fundamental importance in the pursuit of more active and robust WOCs.[15] Evidence of a high-valent ruthenium(V)–oxo intermediate, derived from complex **4**, was found by high-resolution mass spectrometry (Figure 3). This species is regarded as the active key intermediate in the oxidation of

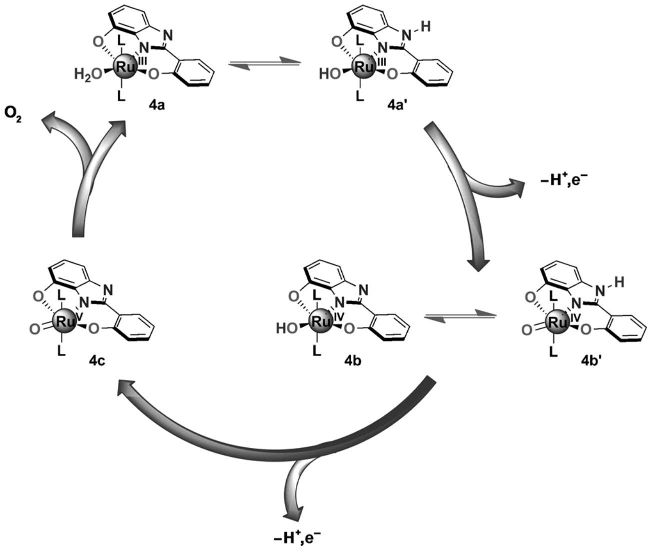

Scheme 2. Possible ligand involvement during water oxidation catalysis mediated by ligand **1** and **2**.

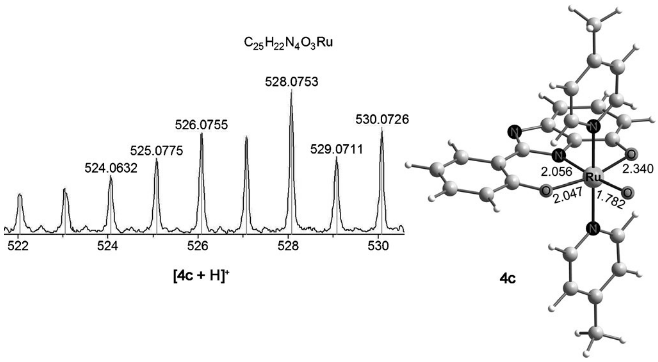

Figure 3. High-resolution mass spectra of the $[Ru^V{=}O]$ of complex **4**, a possible key intermediate in water oxidation, obtained upon the addition of 10 equiv of the oxidant $[Ru(bpy)_3]^{3+}$, and the calculated structure.

water for a variety of ruthenium based WOCs. Complexes **3** and **4** were each mixed with an excess (10 equiv) of the one-electron oxidant $[Ru(bpy)_3]^{3+}$. Aliquots were analyzed periodically by mass spectrometry. Although the mass spectra proved to be complicated, a signal at $m/z = 528.0753$ was observed in positive mode for complex **4**, and assigned to $[Ru^V{=}O\ (\mathbf{4c}) + H^+]^+$. The observed isotope pattern matches with the proposed structure of $[Ru^V{=}O]$. A similar signal could also be obtained for complex **3**. To provide support that complexes **3** and **4** retain their identities after catalytic cycling, additional experiments were carried out. The reaction mixtures for complexes **3** and **4** were analyzed after the addition of 100 equiv of $[Ru(bpy)_3]^{3+}$. For complex **3**, a signal at $m/z = 558.0815$ was found, which corresponds to the aqua complex (**3a**) of complex **3** (Figure S29). For complex **4**, a signal corresponding to the loss of one picoline could be observed ($m/z = 512.0781$).

In summary, the use of molecular catalysts offers the possibility of designing well-defined WOCs that contain high-valent, redox-active metal centers, a key element for oxidizing water. Thus far, the majority of the catalysts developed suffer from the drawback of requiring high redox potentials to oxidize water. Only a few of these complexes are able of carrying out photocatalytic water oxidation. Combining both redox and proton transfer mediator motifs into the WOC would facilitate the simultaneous transfer of electrons and protons, thus avoiding high-energy intermediates and giving access to new reaction pathways. To both decrease the redox potentials and permit coupled proton–electron transfer, imidazole and carboxylate were introduced as mediators into the ligands. Indeed, by introducing the redox and proton transfer mediator motif (imidazole) the WOCs were able to catalyze water oxidation, under neutral conditions, both by pre-generated and photogenerated $[Ru(bpy)_3]^{3+}$. Electrochemical and quantum chemical studies confirmed the interesting redox properties of these complexes. The details of how electrons and protons are transferred in the splitting of water are the fundamental core of understanding and realizing sustainable artificial energy conversion. These catalysts bring us one step closer to achieving artificial photosynthesis by virtue of the potential they have in terms of synthetic ease, cost, high catalytic activity, and the possibility of designing molecular assemblies where they can be coupled to co-catalysts or photosensitizers in light-harvesting water splitting devices.

Received: March 7, 2012

Keywords: electrochemistry · homogeneous catalysis · photocatalysis · ruthenium · water oxidation

---

[1] a) J. Barber, *Chem. Soc. Rev.* **2009**, *38*, 185–196; b) J. K. Hurst, *Science* **2010**, *328*, 315–316.

[2] Y. Umena, K. Kawakami, J.-R. Shen, N. Kamiya, *Nature* **2011**, *473*, 55–60.

[3] a) S. W. Gersten, G. J. Samuels, T. J. Meyer, *J. Am. Chem. Soc.* **1982**, *104*, 4029–4030; b) H.-W. Tseng, R. Zong, J. T. Muckerman, R. Thummel, *Inorg. Chem.* **2008**, *47*, 11763–11773; c) L. Duan, A. Fischer, Y. Xu, L. Sun, *J. Am. Chem. Soc.* **2009**, *131*, 10397–10399; d) M. Yoshida, S. Masaoka, K. Sakai, *Chem. Lett.* **2009**, *38*, 702–703; e) J. J. Concepcion, J. W. Jurss, M. R. Norris, Z. Chen, J. L. Templeton, T. J. Meyer, *Inorg. Chem.* **2010**, *49*, 1277–1279; f) J. Nyhlén, L. Duan, B. Åkermark, L. Sun, T. Privalov, *Angew. Chem.* **2010**, *122*, 1817–1821; *Angew. Chem. Int. Ed.* **2010**, *49*, 1773–1777; g) S. Roeser, P. Farràs, F. Bozoglian, M. Martínez-Belmonte, J. Benet-Buchholz, A. Llobet, *ChemSusChem* **2011**, *4*, 197–207; h) T. Privalov, B. Åkermark, L. Sun, *Chem. Eur. J.* **2011**, *17*, 8313–8317; i) M. Murakami, D. Hong, T. Suenobu, S. Yamaguchi, T. Ogura, S. Fukuzumi, *J. Am. Chem. Soc.* **2011**, *133*, 11605–11613; j) Y. Xu, A. Fisher, L. Duan, L. Tong, E. Gabrielsson, B. Åkermark, L. Sun, *Angew. Chem.* **2010**, *122*, 9118–9121; *Angew. Chem. Int. Ed.* **2010**, *49*, 8934–8937.

[4] a) N. D. McDaniel, F. J. Coughlin, L. L. Tinker, S. Bernhard, *J. Am. Chem. Soc.* **2008**, *130*, 210–217; b) J. F. Hull, D. Balcells, J. D. Blakemore, C. D. Incarvito, O. Eisenstein, G. W. Brudvig, R. H. Crabtree, *J. Am. Chem. Soc.* **2009**, *131*, 8730–8731; c) W. I. Dzik, S. E. Calvo, J. N. H. Reek, M. Lutz, M. A. Ciriano, C. Tejel, D. G. H. Hetterscheid, B. de Bruin, *Organometallics* **2011**, *30*, 372–374.

[5] a) R. Brimblecombe, A. Koo, G. C. Dismukes, G. F. Swiegers, L. Spiccia, *J. Am. Chem. Soc.* **2010**, *132*, 2892–2894; b) E. A. Karlsson, B.-L. Lee, T. Åkermark, E. V. Johnston, M. D. Kärkäs, J. Sun, Ö. Hansson, J.-E. Bäckvall, B. Åkermark, *Angew. Chem.* **2011**, *123*, 11919–11922; *Angew. Chem. Int. Ed.* **2011**, *50*, 11715–11718.

[6] a) M. W. Kanan, D. G. Nocera, *Science* **2008**, *321*, 1072–1075; b) Q. Yin, J. Miles Tan, C. Besson, Y. V. Geletii, D. G. Musaev, A. E. Kuznetsov, Z. Luo, K. I. Hardcastle, C. L. Hill, *Science* **2010**, *328*, 342–345; c) D. J. Wasylenko, C. Ganesamoorthy, J. Borau-Garcia, C. P. Berlinguette, *Chem. Commun.* **2011**, *47*, 4249–4251; d) Z. Huang, Z. Luo, Y. V. Geletii, J. W. Vickers, Q. Yin, D. Wu, Y. Hou, Y. Ding, J. Song, D. G. Musaev, C. L. Hill, T. Lian, *J. Am. Chem. Soc.* **2011**, *133*, 2068–2071.

[7] a) W. C. Ellis, N. D. McDaniel, S. Bernhard, T. J. Collins, *J. Am. Chem. Soc.* **2010**, *132*, 10990–10991; b) J. L. Fillol, Z. Codolà, I. Garcia-Bosch, L. Gómez, J. J. Pla, M. Costas, *Nat. Chem.* **2011**, *3*, 807–813.

[8] a) T. J. Meyer, M. H. V. Huynh, H. Holden Thorp, *Angew. Chem.* **2007**, *119*, 5378–5399; *Angew. Chem. Int. Ed.* **2007**, *46*, 5284–5304; b) O. S. Wenger, *Chem. Eur. J.* **2011**, *17*, 11692–11702.

[9] Y. V. Geletii, B. Botar, P. Kögerler, D. A. Hillesheim, D. G. Musaev, C. L. Hill, *Angew. Chem.* **2008**, *120*, 3960–3963; *Angew. Chem. Int. Ed.* **2008**, *47*, 3896–3899.

[10] L. Duan, Y. Xu, P. Zhang, M. Wang, L. Sun, *Inorg. Chem.* **2010**, *49*, 209–215.

[11] F. Bolletta, A. Juris, M. Maestri, D. Sandrini, *Inorg. Chim. Acta* **1980**, *44*, L175–L176.

[12] a) J. Limburg, J. S. Vrettos, L. M. Liable-Sands, A. L. Rheingold, R. H. Crabtree, G. W. Brudvig, *Science* **1999**, *283*, 1524–1527; b) Y. Shimazaki, T. Nagano, H. Takesue, B.-H. Ye, F. Tani, Y. Naruta, *Angew. Chem.* **2004**, *116*, 100–102; *Angew. Chem. Int. Ed.* **2004**, *43*, 98–100; c) A. K. Poulsen, A. Rompel, C. J. McKenzie, *Angew. Chem.* **2005**, *117*, 7076–7080; *Angew. Chem. Int. Ed.* **2005**, *44*, 6916–6920.

[13] See the Supporting Information for details.

[14] An agreement between the electron density distributions computed with vastly different density functionals, indicates that such a delocalization is not a computational artifact.

[15] a) J. J. Concepcion, M.-K. Tsai, J. T. Muckerman, T. J. Meyer, *J. Am. Chem. Soc.* **2010**, *132*, 1545–1557; b) D. E. Polyansky, J. T. Muckerman, J. Rochford, R. Zong, R. P. Thummel, E. Fujita, *J. Am. Chem. Soc.* **2011**, *133*, 14649–14665; c) A. Kimoto, K. Yamauchi, M. Yoshida, S. Masaoka, K. Sakai, *Chem. Commun.* **2012**, *48*, 239–241.